

Circular-Polarization Reconfigurable Monopole Antenna with Enhanced Boresight Gain for GNSS Applications

Y.F. Cao, S.W. Cheung, and T.I. Yuk

Department of Electrical and Electronic Engineering, The University of Hong Kong, Hong Kong
[yfcao, swcheung, tiyuk]@eee.hku.hk

Abstract—A circular-polarization (CP) reconfigurable monopole antenna with enhanced boresight-gain for GNSS applications is proposed. The antenna consists of two meandered monopoles placed perpendicular to each other, a feeding network using the Wilkinson power divider, two switchable 90°-phase-shifters, a defected ground structure (DGS) and a metallic reflector. The metallic reflector is placed at the back of the antenna to improve efficiency and boresight gain. Simulation results show that the metallic reflector can substantially increase the efficiency and boresight-gain of the antenna by about 20% and 5 dB, respectively, in the operating band, yet retaining the impedance bandwidth and axial-ratio bandwidth.

Index Terms—polarization reconfigurable, monopole antenna, GNSS, reflector, biasing circuit, boresight gain enhancement.

I. INTRODUCTION

Reconfigurable antennas have received much attention and been designed using different techniques [1-6]. Polarization-reconfigurable antennas are attractive in different applications such as multiple-input–multiple-output (MIMO) systems [7], synthetic-aperture radar, and frequency reuses [8]. In the past, polarization-reconfigurable antennas were usually designed using patch [9-11] and slot [12-14] antennas. For the patch antenna in [3], PIN-diode switches placed on the patch radiators were used to change the radiator shapes and hence to switch between right- and left-handed circular polarizations (RHCP and LHCP). In the patch antenna in [10], switchable slots were etched on the patch radiators to achieve CP reconfiguration. To avoid the effects of biasing circuits on the radiators in [9,10], the CP reconfigurable patch antenna in [11] was designed using switchable slots on the ground plane. For the slot antenna in [12], a PIN diode placed across the radiating slots was switched ON/OFF to realize CP configuration. In [13], CP reconfigurability of a slot antenna was achieved using a switchable feed network on the opposite layer of the radiating slot. In [14], PIN diodes were used to connect with two T-shaped microstrips which were protruded from the ground plane for CP reconfiguration. The biasing circuits for patch and slot antennas are easy to design. However, patch antenna and slot antenna have narrower bandwidths than that of monopole antenna, and they have a theoretical electrical length of half-wavelength which is double the size of

monopole antenna. Thus in [15], a simple polarization-reconfigurable monopole antenna using a novel biasing technique was designed for GNSS/PCS applications. In the design [15], a feed network with two switchable phase shifters was used to change the phase difference between the signals from the two monopole elements, and hence to switch the antenna between RHCP and LHCP. The antenna had a more compact size and wider axial-ratio bandwidth (ARBW, AR < 3 dB) than those in [9-14], but having a very low realized boresight gain of only about 0 dBi.

The CP reconfigurable monopole antenna in [15] had two meandered monopoles as the radiators. In this paper, we propose a simple and effective way, i.e., placing a metallic reflector at the back of the CP antenna, to improve the performance in terms of gain and efficiency of the CP antenna in [15]. The EM simulation software CST is used to study the improvement. Results show that the metallic reflector can substantially enhance the efficiency and gain of the CP antenna by 20% and 5.5 dB, respectively, in the operating band.

II. ANTENNA DESIGN

A. Antenna Structure

The circular-polarization (CP) reconfigurable monopole antenna studied here is shown in Fig. 1, which has a symmetrical structure and consists of two meandered monopoles with microstrip-fed, a Wilkinson power divider, two switchable 90°-phase shifters implemented using two $\lambda_g/4$ -microstrip delay lines, a defected ground structure (DGS) and a reflector. The microstrip-feed lines have a characteristic impedance of $Z_0=50 \Omega$. The Wilkinson power divider is designed using the procedure in [16]. The input signal in Fig. 1(a) is divided into two equal-power signals by the Wilkinson power divider and fed to the phase shifters and then the corresponding meandered monopoles. The two monopoles are placed perpendicular to each other to generate two orthogonal electric-field components [17]. Six PIN diodes ($D1 \& D2 \& D3$ or $D1' \& D2' \& D3'$ as shown in Fig. 1(a)) are used as two switches to determine whether the input signals will go through the corresponding 90°-phase shifters. The biasing circuits for the PIN diodes are used to switch ON/OFF the phase shifters. For RHCP operation, the phase shifter on the

right-hand side (RHS) is turned ON. The signal fed to the RHS monopole will then lead the other signal by 90° , making the antenna RHCP. The LHCP operation is similar to the RHCP operation. Thus the antenna is CP reconfigurable. The DGS on the ground plane is a slot, serving as a $\lambda_g/4$ -slot resonator to reduce mutual coupling between the two monopoles and improve matching. To save space and keep the antenna structure symmetrical, the slot is split into two slots and bent toward both sides as shown in Figs. 1(a) and (c). The slot length is about $L11+2L12+2L13=\lambda_g/4$. A metallic reflector is placed at a distance of about $\lambda_g/4$ from the antenna, as shown in Fig. 1 (b).

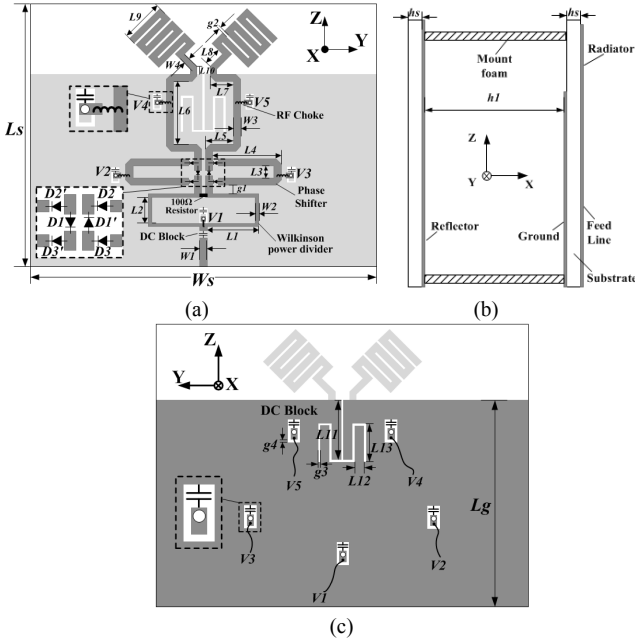


Fig. 1. Geometry of proposed antenna: (a) top view, (b) side view and (c) bottom view (█████ metal in front and ████ metal in bottom)

B. DC Biasing Circuit

The biasing circuits for the six PIN diodes are shown in Fig. 1. In Fig. 1(a), a DC bias voltage $V4$ is provided to the anodes of diodes $D1$, and $D2'$ through a DC pad which is connected to the feed line via an inductor (LQW15A with value 82 nH from Murata) for RF isolation. In Fig. 1(b), another DC pad is created in exactly the same position on the other side of the substrate which is RF coupled to the ground plane using a capacitor with value 100 pF. The two DC pads are connected together through a via and so are RF grounded. A DC voltage $V2$ is supplied to the cathodes of diodes $D2'$ and $D3'$, and a DC voltage $V1$ is supplied to diode $D1$ using the similar method. The antenna on the RHS is just mirror imaging of the LHS, so the biasing technique and operations are about the same. The practical PIN diodes (BAR50-02V, SC-79) from Infineon is used and the diode has a forward DC voltage of 0.95 V [18]. For simulation, the models of the PIN diodes as shown in Fig. 2 are used [18].

The CP reconfigurable antenna is designed on a Rogers RO 4350 substrate with an area of 88×67 mm 2 , a relative

permittivity of 3.66 and a loss tangent of 0.004. The dimensions of the final design are listed in Table I.

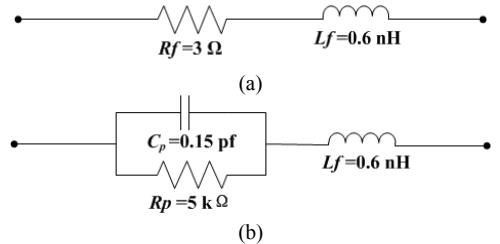


Fig. 2. Simulation models of PIN diode in (a) “ON” and (b) “OFF” states

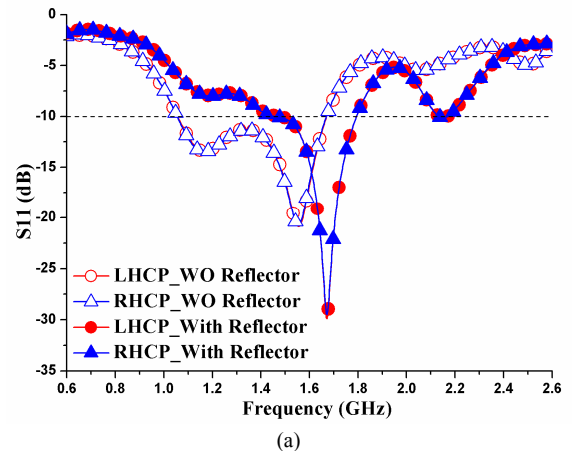
TABLE I. DIMENSIONS OF PROPOSED RECONFIGURATION ANTENNA (MM)

$L1$	$L2$	$L3$	$L4$	$L5$	$L6$	$L7$	$L8$	$L9$
11.0	7.0	3.0	13.8	7.2	16.0	6.0	4.5	12.0
$L10$	$L11$	$L12$	$L13$	$g1$	$g2$	$g3$	$g4$	$W1$
2.0	13.7	2.3	7.0	2.0	0.6	0.4	0.4	1.8
$W2$	$W3$	$W4$	$W5$	hs	$h1$	Ls		
0.9	1.8	1.6	88.0	0.8	35.0	67.0		

III. SIMULATION AND DISCUSSIONS

A. S11 and AR

The simulated S11 and AR with and without using the metallic reflector are shown in Fig. 3. Without using the reflector, Fig. 3(a) shows that the impedance bandwidth for $S11 < -10$ dB is 1.06-1.67 GHz, and Fig. 3(b) shows that the ARBW for $AR < 3$ dB is from 1.43 to 1.83 GHz. Thus the antenna has an operating frequency band of 1.43-1.67 GHz which can be used for the GNSS system. With the use of the reflector, Fig. 3(a) shows that the impedance bandwidth is 1.46-1.79 GHz, about half of that without using the reflector, and Fig. 3(b) shows that the ARBW is 1.5-1.9 GHz, about the same as that without using the reflector. Thus the antenna has an operating band of 1.5-1.79 GHz which is enough for the GNSS system.



(a)

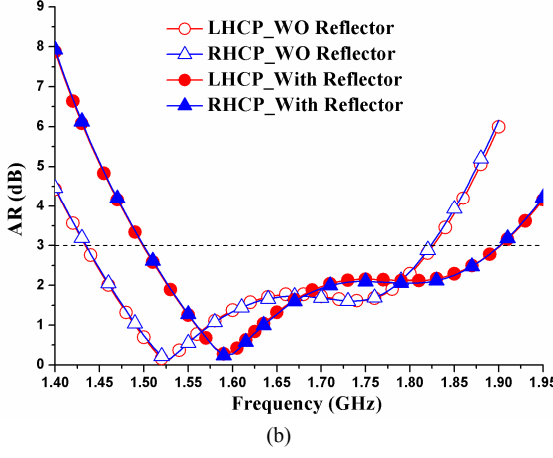


Fig. 3. Simulated (a) S11 and (b) AR with and without the reflector

The ARs with different elevation and azimuth angles have also been studied using simulation. The results in the x-z and x-y planes are shown in Figs. 4(a) and (b), respectively. Without the reflector and in the x-z plane, Fig. 4(a) shows that the simulated AR is less than 3 dB for $65^\circ < \theta < 138^\circ$ and $-138^\circ < \theta < -65^\circ$ in both RHCP and LHCP. In the x-y plane, Fig. 4(b) shows that the simulated AR is less than 3 dB for $-38^\circ < \phi < 25^\circ$ in RHCP and $-25^\circ < \phi < 38^\circ$ in LHCP. Thus the antenna has the beamwidths of about 70° in the x-z plane and 60° in the x-y plane (for AR<3 dB) in the boresight direction ($\theta=90^\circ, \phi=0^\circ$) in both RHCP and LHCP. With the use of the reflector and in the x-z plane, Fig. 4(a) shows that the simulated AR is less than 3 dB for $50^\circ < \theta < 130^\circ$ and $-46^\circ < \theta < -29^\circ$ in both RHCP and LHCP. In the x-y plane, Fig. 4(b) shows that the simulated AR is less than 3 dB for $-48^\circ < \phi < 24^\circ$ in RHCP and $-24^\circ < \phi < 48^\circ$ in LHCP. In both RHCP and LHCP, the antenna now has the increased beamwidths of about 80° (for AR < 3 dB) in the x-z plane and 70° in the x-y plane in the boresight direction. The AR beamwidths in the opposite boresight directions are reduced substantially and also shifted.

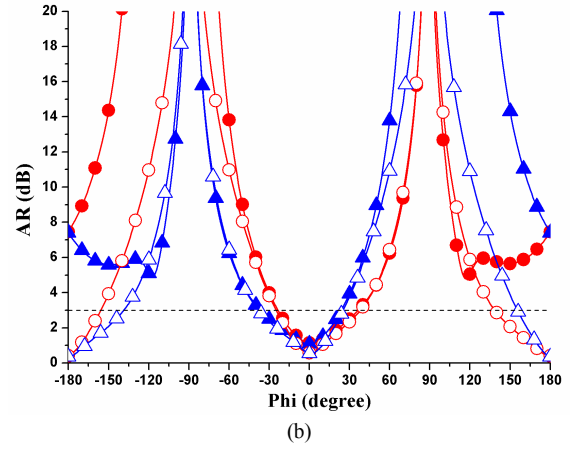
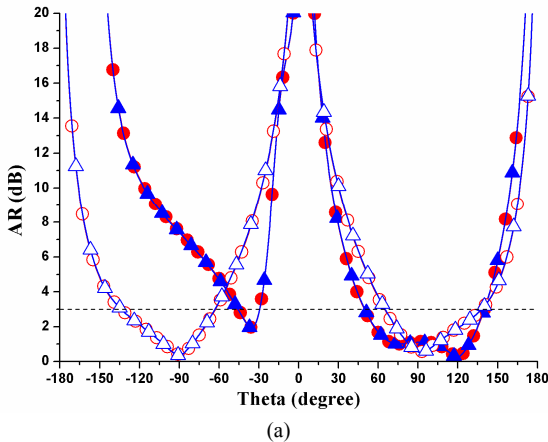


Fig. 4. Simulated AR in (a) x-z plane and (b) x-y plane at corresponding center frequency with and without using reflector (Antenna in RHCP: \blacktriangle and LHCP: \bullet with reflector at 1.64 GHz; Antenna in RHCP: \triangle and LHCP: \circ without reflector at 1.55 GHz)

B. Radiation Patterns

Fig. 5 shows the simulated radiation patterns of realized gain in CP with and without the use of the reflector. Again, the center frequency of 1.55 GHz is used for the case without using the reflector and 1.64 GHz for the case with using the reflector. Fig. 5(s) shows that, in RHCP, the radiation patterns of co-polarization point at the $+x$ direction and have a null at the $-x$ direction. The radiation patterns of cross-polarization point at the $-x$ direction and have a null at the $+x$ direction. In LHCP, Fig. 5(b) shows that the radiation patterns are in the opposite directions to those in Fig. 5(a). It is clear from Fig. 5 that the antenna with the reflector has a higher boresight gain at $\phi=0^\circ$ and $\theta=90^\circ$ than the case without the reflector.

C. Efficiency and Boresight gain

Fig. 6 shows the simulated efficiency of the antenna with and without the reflector. Without the reflector, the efficiency of the antenna is less than 60% across the operating band in both RHCP and LHCP. However, the efficiency of the proposed antenna with the reflector is much higher across the operating band, ranging from 62% to 82.3% in both RHCP and LHCP. Fig. 7 shows the realized boresight gain with and without the reflector. The simulated realized boresight gain without reflector is only about 0 dBi as shown in Fig. 7(a). With the reflector, the gain in co-polarization is much higher, ranging from 2.7 to 5.5 dBi as shown in Fig. 7(b). At the frequency of 1.575 GHz (the center frequency for the GNSS system), the efficiency and boresight gain are increased by about 20% and 5 dB, respectively. Although cross-polarization is also slightly higher in both RHCP and LHCP, it is lower than -10 dBi.

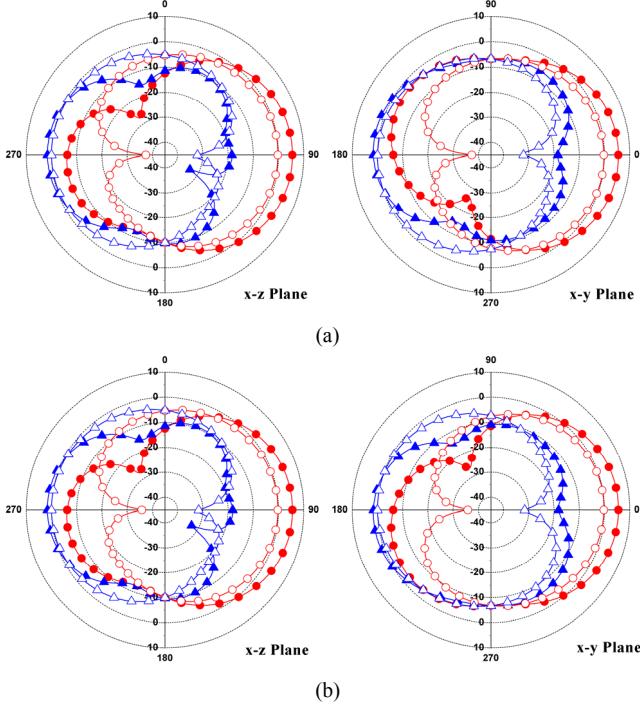


Fig. 5. Simulated radiation patterns of antenna in (a) RHCP configuration and (b) LHCP configuration with and without reflector (—▲— cross-polarization, ●—●— co-polarization with reflector at 1.64 GHz; —○— cross-polarization, —○— co-polarization without reflector at 1.55 GHz)

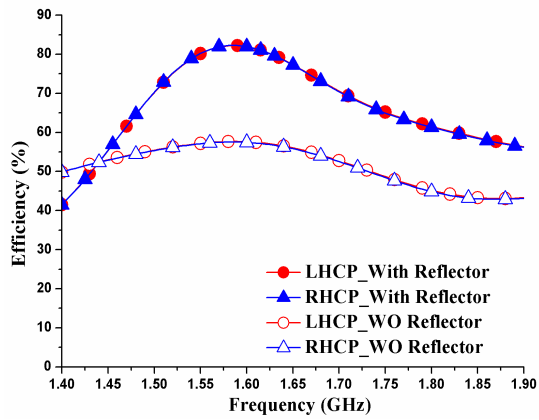


Fig. 6. Simulated efficiency with and without the reflector

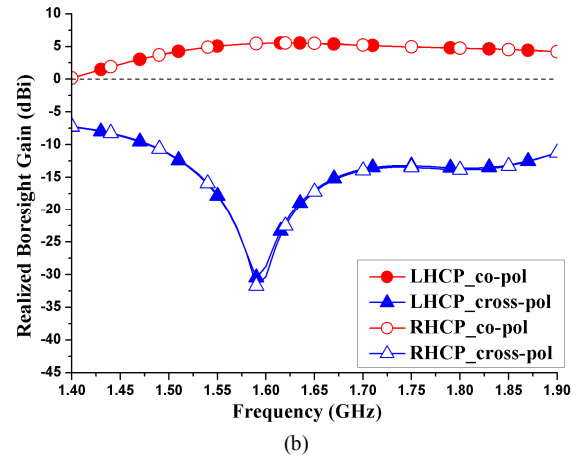
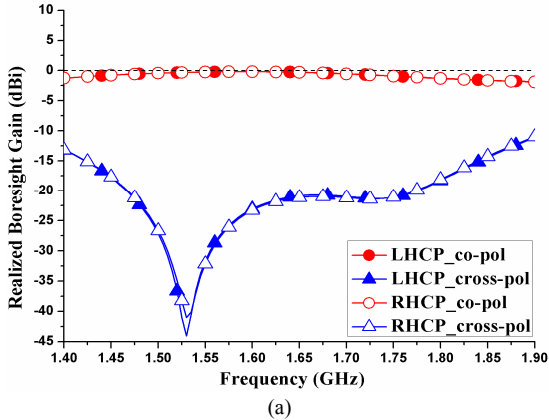


Fig. 7. Simulated realized boresight gain (a) without (b) with the reflector of the proposed antenna

IV. CONCLUSIONS

A simple way to improve the efficiency and boresight gain of a CP reconfigurable monopole antenna for GNSS applications has been proposed and studied. A metallic reflector is placed at the back of the antenna to improve the performance of the antenna. Simulated results have shown that, by using the metallic reflector, the efficiency and boresight gain can be increased by about 20% and 5 dB, respectively, yet the impedance bandwidth and ARBW remaining about the same.

REFERENCES

- [1] Y. F. Cao, S. W. Cheung, X. L. Sun and T. I. Yuk, "Frequency-reconfigurable monopole antenna with wide tuning range for cognitive radio," *Microw. Opt. Tech. Lett.*, vol. 56, no. 1, pp. 145-152, Jan. 2014.
- [2] H. L. Zhu, X. H. Liu, S. W. Cheung and T. I. Yuk, "Frequency-reconfigurable antenna using metasurface," *IEEE Trans. Antennas Propag.*, vol. 62, no. 1, pp. 80-85, Jan. 2014.
- [3] H. L. Zhu, S. W. Cheung, X. H. Liu and T. I. Yuk, "Design of polarization reconfigurable antenna using metasurface," *IEEE Trans. Antennas Propag.*, vol. 62, no. 6, pp. 2891-2898, Jun. 2014.
- [4] X. L. Sun, S. W. Cheung and T. I. Yuk, "Dual-band monopole antenna with frequency-tunable feature for wimax applications," *IEEE Antennas Wireless Propag. Lett.*, vol. 12, pp. 100-103, 2013.
- [5] H. F. Abutarboush, R. Nilavalan, S. W. Cheung, K. Nasr, T. Peter and D. Budimir, "A reconfigurable wideband and multiband antenna using dual-patch elements for compact wireless devices," *IEEE Trans. Antennas Propag.*, vol. 60, no. 1, pp. 36-43, Jan. 2012.
- [6] H. F. Abutarboush, R. Nilavalan, S. W. Cheung and K. Nasr, "Compact printed multiband antenna with independent setting suitable for fixed and reconfigurable wireless communication systems," *IEEE Trans. Antennas Propag.*, vol. 60, no. 8, pp. 3867-3874, Aug. 2012.
- [7] S. Gao, A. Sambell, and S. S. Zhong, "Polarization-agile antennas," *IEEE Antennas Propag. Mag.*, vol. 48, no. 3, pp. 28-37, Jun. 2006.
- [8] P. Y. Qin, Y. J. Guo, and C. H. Liang, "Effect of antenna polarization diversity on MIMO system capacity," *IEEE Antennas Wireless Propag. Lett.*, vol. 9, pp. 1092-1095, 2010.
- [9] Y. Sung, "Investigation into the polarization of asymmetrical feed triangular microstrip antennas and its application to reconfigurable antennas," *IEEE Trans. Antennas Propag.*, vol. 58, no. 4, pp. 1039-1046, Apr. 2010.

- [10] S. Pyo, J. W. Baik and Y. S. Kim, "Slot-perturbed microstrip antenna for switchable circular polarization," *Electron Lett.*, vol. 47 no. 10, pp. 583-585, May. 2011.
- [11] X. X. Yang, B. C. Shao, F. Yang, A. Z. Elsherbeni, and B. Gong, "A polarization reconfigurable patch antenna with loop slots on the ground plane," *IEEE Antennas Wireless Propag. Lett.*, vol. 11, pp. 69-72, 2012.
- [12] W. M. Dorsey, A. I. Zaghloul, and M. G. Parent, "Perturbed square-ring slot antenna with reconfigurable polarization," *IEEE Antennas Wireless Propag. Lett.*, vol. 8, pp. 603-606, 2009.
- [13] J. S. Row, W. L. Liu, and T. R. Chen, "Circular polarization and polarization reconfigurable designs for annular slot antennas," *IEEE Trans. Antennas Propag.*, vol. 60, no. 12, pp. 5998-6002, Dec. 2012.
- [14] Y. B. Chen, Y. C. Jiao, and F. S. Zhang, "Polarization reconfigurable CPW-fed square slot antenna using pin diodes," *Microw. Opt. Tech. Lett.*, vol. 49, no. 6, pp. 1233-1236, Jun. 2007.
- [15] Y. F. Cao, S. W. Cheung, and T. I. Yuk, "A simple planar polarization reconfigurable monopole antenna for GNSS/PCS," accepted by *IEEE Trans. Antennas Propag.*.
- [16] D. M. Pozar, "Microwave engineering," John Wiley & Sons, (4th Edition), 2012, ch. 7, pp. 328-332.
- [17] C. A. Balanis, "Antenna theory - analysis and design," John Wiley & Sons, (3rd Edition), 2005, ch. 2, pp. 73-74.
- [18] Datasheet for bar50series, Infineon Technologies AG81726 Munich, Germany, Jul 2011.